

Measurement of the Top Quark Mass Using Dilepton Events

B. Abbott,²⁸ M. Abolins,²⁵ B. S. Acharya,⁴³ I. Adam,¹² D. L. Adams,³⁷ M. Adams,¹⁷ S. Ahn,¹⁴ H. Aihara,²² G. A. Alves,¹⁰ E. Amidi,²⁹ N. Amos,²⁴ E. W. Anderson,¹⁹ R. Astur,⁴² M. M. Baarmand,⁴² A. Baden,²³ V. Balamurali,³² J. Balderston,¹⁶ B. Baldin,¹⁴ S. Banerjee,⁴³ J. Bantly,⁵ E. Barberis,²² J. F. Bartlett,¹⁴ K. Bazizi,³⁹ A. Belyaev,²⁶ S. B. Beri,³⁴ I. Bertram,³¹ V. A. Bezzubov,³⁵ P. C. Bhat,¹⁴ V. Bhatnagar,³⁴ M. Bhattacharjee,¹³ N. Biswas,³² G. Blazey,³⁰ S. Blessing,¹⁵ P. Bloom,⁷ A. Boehnlein,¹⁴ N. I. Bojko,³⁵ F. Borchering,¹⁴ J. Borders,³⁹ C. Boswell,⁹ A. Brandt,¹⁴ R. Brock,²⁵ A. Bross,¹⁴ D. Buchholz,³¹ V. S. Burtovoi,³⁵ J. M. Butler,³ W. Carvalho,¹⁰ D. Casey,³⁹ Z. Casilum,⁴² H. Castilla-Valdez,¹¹ D. Chakraborty,⁴² S.-M. Chang,²⁹ S. V. Chekulaev,³⁵ L.-P. Chen,²² W. Chen,⁴² S. Choi,⁴¹ S. Chopra,²⁴ B. C. Choudhary,⁹ J. H. Christenson,¹⁴ M. Chung,¹⁷ D. Claes,²⁷ A. R. Clark,²² W. G. Cobau,²³ J. Cochran,⁹ W. E. Cooper,¹⁴ C. Cretsinger,³⁹ D. Cullen-Vidal,⁵ M. A. C. Cummings,¹⁶ D. Cutts,⁵ O. I. Dahl,²² K. Davis,² K. De,⁴⁴ K. Del Signore,²⁴ M. Demarteau,¹⁴ D. Denisov,¹⁴ S. P. Denisov,³⁵ H. T. Diehl,¹⁴ M. Diesburg,¹⁴ G. Di Loreto,²⁵ P. Draper,⁴⁴ Y. Ducros,⁴⁰ L. V. Dudko,²⁶ S. R. Dugad,⁴³ D. Edmunds,²⁵ J. Ellison,⁹ V. D. Elvira,⁴² R. Engelmann,⁴² S. Eno,²³ G. Eppley,³⁷ P. Ermolov,²⁶ O. V. Eroshin,³⁵ V. N. Evdokimov,³⁵ T. Fahland,⁸ M. Fatyga,⁴ M. K. Fatyga,³⁹ J. Featherly,⁴ S. Feher,¹⁴ D. Fein,² T. Ferbel,³⁹ G. Finocchiaro,⁴² H. E. Fisk,¹⁴ Y. Fisyak,⁷ E. Flattum,¹⁴ G. E. Forden,² M. Fortner,³⁰ K. C. Frame,²⁵ S. Fuess,¹⁴ E. Gallas,⁴⁴ A. N. Galyaev,³⁵ P. Gartung,⁹ T. L. Geld,²⁵ R. J. Genik, II,²⁵ K. Genser,¹⁴ C. E. Gerber,¹⁴ B. Gibbard,⁴ S. Glenn,⁷ B. Gobbi,³¹ M. Goforth,¹⁵ A. Goldschmidt,²² B. Gómez,¹ G. Gómez,²³ P. I. Goncharov,³⁵ J. L. González Solís,¹¹ H. Gordon,⁴ L. T. Goss,⁴⁵ K. Gounder,⁹ A. Goussiou,⁴² N. Graf,⁴ P. D. Grannis,⁴² D. R. Green,¹⁴ J. Green,³⁰ H. Greenlee,¹⁴ G. Grim,⁷ S. Grinstein,⁶ N. Grossman,¹⁴ P. Grudberg,²² S. Grünendahl,³⁹ G. Guglielmo,³³ J. A. Guida,² J. M. Guida,⁵ A. Gupta,⁴³ S. N. Gurzhiev,³⁵ P. Gutierrez,³³ Y. E. Gutnikov,³⁵ N. J. Hadley,²³ H. Haggerty,¹⁴ S. Hagopian,¹⁵ V. Hagopian,¹⁵ K. S. Hahn,³⁹ R. E. Hall,⁸ S. Hansen,¹⁴ J. M. Hauptman,¹⁹ D. Hedin,³⁰ A. P. Heinson,⁹ U. Heintz,¹⁴ R. Hernández-Montoya,¹¹ T. Heuring,¹⁵ R. Hirosky,¹⁵ J. D. Hobbs,¹⁴ B. Hoeneisen,^{1,*} J. S. Hoftun,⁵ F. Hsieh,²⁴ Ting Hu,⁴² Tong Hu,¹⁸ T. Huehn,⁹ A. S. Ito,¹⁴ E. James,² J. Jaques,³² S. A. Jerger,²⁵ R. Jesik,¹⁸ J. Z.-Y. Jiang,⁴² T. Joffe-Minor,³¹ K. Johns,² M. Johnson,¹⁴ A. Jonckheere,¹⁴ M. Jones,¹⁶ H. Jöstlein,¹⁴ S. Y. Jun,³¹ C. K. Jung,⁴² S. Kahn,⁴ G. Kalbfleisch,³³ J. S. Kang,²⁰ R. Kehoe,³² M. L. Kelly,³² C. L. Kim,²⁰ S. K. Kim,⁴¹ A. Klatchko,¹⁵ B. Klima,¹⁴ C. Klopfenstein,⁷ V. I. Klyukhin,³⁵ V. I. Kochetkov,³⁵ J. M. Kohli,³⁴ D. Koltick,³⁶ A. V. Kostitskiy,³⁵ J. Kotcher,⁴ A. V. Kotwal,¹² J. Kourlas,²⁸ A. V. Kozelov,³⁵ E. A. Kozlovski,³⁵ J. Krane,²⁷ M. R. Krishnaswamy,⁴³ S. Krzywdzinski,¹⁴ S. Kunori,²³ S. Lami,⁴² H. Lan,^{14,†} R. Lander,⁷ F. Landry,²⁵ G. Landsberg,¹⁴ B. Lauer,¹⁹ A. Leflat,²⁶ H. Li,⁴² J. Li,⁴⁴ Q. Z. Li-Demarteau,¹⁴ J. G. R. Lima,³⁸ D. Lincoln,²⁴ S. L. Linn,¹⁵ J. Linnemann,²⁵ R. Lipton,¹⁴ Q. Liu,^{14,†} Y. C. Liu,³¹ F. Lobkowicz,³⁹ S. C. Loken,²² S. Lökös,⁴² L. Lueking,¹⁴ A. L. Lyon,²³ A. K. A. Maciel,¹⁰ R. J. Madaras,²² R. Madden,¹⁵ L. Magaña-Mendoza,¹¹ S. Mani,⁷ H. S. Mao,^{14,†} R. Markeloff,³⁰ L. Markosky,² T. Marshall,¹⁸ M. I. Martin,¹⁹ K. M. Mauritz,¹⁹ B. May,³¹ A. A. Mayorov,³⁵ R. McCarthy,⁴² J. McDonald,¹⁵ T. McKibben,¹⁷ J. McKinley,²⁵ T. McMahon,³³ H. L. Melanson,¹⁴ M. Merkin,²⁶ K. W. Merritt,¹⁴ H. Miettinen,³⁷ A. Mincer,²⁸ J. M. de Miranda,¹⁰ C. S. Mishra,¹⁴ N. Mokhov,¹⁴ N. K. Mondal,⁴³ H. E. Montgomery,¹⁴ P. Mooney,¹ H. da Motta,¹⁰ C. Murphy,¹⁷ F. Nang,² M. Narain,¹⁴ V. S. Narasimham,⁴³ A. Narayanan,² H. A. Neal,²⁴ J. P. Negret,¹ P. Nemethy,²⁸ M. Nicola,¹⁰ D. Norman,⁴⁵ L. Oesch,²⁴ V. Oguri,³⁸ E. Oltman,²² N. Oshima,¹⁴ D. Owen,²⁵ P. Padley,³⁷ M. Pang,¹⁹ A. Para,¹⁴ Y. M. Park,²¹ R. Partridge,⁵ N. Parua,⁴³ M. Paterno,³⁹ J. Perkins,⁴⁴ M. Peters,¹⁶ R. Piegaia,⁶ H. Piekarczyk,¹⁵ Y. Pischalnikov,³⁶ V. M. Podstavkov,³⁵ B. G. Pope,²⁵ H. B. Prosper,¹⁵ S. Protopopescu,⁴ J. Qian,²⁴ P. Z. Quintas,¹⁴ R. Raja,¹⁴ S. Rajagopalan,⁴ O. Ramirez,¹⁷ L. Rasmussen,⁴² S. Reucroft,²⁹ M. Rijssenbeek,⁴² T. Rockwell,²⁵ N. A. Roe,²² P. Rubinov,³¹ R. Ruchti,³² J. Rutherford,² A. Sánchez-Hernández,¹¹ A. Santoro,¹⁰ L. Sawyer,⁴⁴ R. D. Schamberger,⁴² H. Schellman,³¹ J. Sculli,²⁸ E. Shabalina,²⁶ C. Shaffer,¹⁵ H. C. Shankar,⁴³ R. K. Shivpuri,¹³ M. Shupe,² H. Singh,⁹ J. B. Singh,³⁴ V. Sirotenko,³⁰ W. Smart,¹⁴ A. Smith,² R. P. Smith,¹⁴ R. Snihur,³¹ G. R. Snow,²⁷ J. Snow,³³ S. Snyder,⁴ J. Solomon,¹⁷ P. M. Sood,³⁴ M. Sosebee,⁴⁴ N. Sotnikova,²⁶ M. Souza,¹⁰ A. L. Spadafora,²² R. W. Stephens,⁴⁴ M. L. Stevenson,²² D. Stewart,²⁴ D. A. Stoianova,³⁵ D. Stoker,⁸ M. Strauss,³³ K. Streets,²⁸ M. Strovink,²² A. Sznajder,¹⁰ P. Tamburello,²³ J. Tarazi,⁸ M. Tartaglia,¹⁴ T. L. T. Thomas,³¹ J. Thompson,²³ T. G. Trippe,²² P. M. Tuts,¹² N. Varelas,²⁵ E. W. Varnes,²² D. Vitoe,² A. A. Volkov,³⁵ A. P. Vorobiev,³⁵ H. D. Wahl,¹⁵ G. Wang,¹⁵ J. Warchol,³² G. Watts,⁵ M. Wayne,³² H. Weerts,²⁵ A. White,⁴⁴ J. T. White,⁴⁵ J. A. Wightman,¹⁹ S. Willis,³⁰ S. J. Wimpenny,⁹ J. V. D. Wirjawan,⁴⁵ J. Womersley,¹⁴ E. Won,³⁹

D. R. Wood,²⁹ H. Xu,⁵ R. Yamada,¹⁴ P. Yamin,⁴ C. Yanagisawa,⁴² J. Yang,²⁸ T. Yasuda,²⁹ P. Yepes,³⁷ C. Yoshikawa,¹⁶
S. Youssef,¹⁵ J. Yu,¹⁴ Y. Yu,⁴¹ Z. H. Zhu,³⁹ D. Zieminska,¹⁸ A. Zieminski,¹⁸ E. G. Zverev,²⁶ and A. Zylberstejn⁴⁰

(D0 Collaboration)

¹Universidad de los Andes, Bogotá, Colombia

²University of Arizona, Tucson, Arizona 85721

³Boston University, Boston, Massachusetts 02215

⁴Brookhaven National Laboratory, Upton, New York 11973

⁵Brown University, Providence, Rhode Island 02912

⁶Universidad de Buenos Aires, Buenos Aires, Argentina

⁷University of California, Davis, California 95616

⁸University of California, Irvine, California 92697

⁹University of California, Riverside, California 92521

¹⁰LAFEX, Centro Brasileiro de Pesquisas Físicas, Rio de Janeiro, Brazil

¹¹CINVESTAV, Mexico City, Mexico

¹²Columbia University, New York, New York 10027

¹³Delhi University, Delhi, India 110007

¹⁴Fermi National Accelerator Laboratory, Batavia, Illinois 60510

¹⁵Florida State University, Tallahassee, Florida 32306

¹⁶University of Hawaii, Honolulu, Hawaii 96822

¹⁷University of Illinois at Chicago, Chicago, Illinois 60607

¹⁸Indiana University, Bloomington, Indiana 47405

¹⁹Iowa State University, Ames, Iowa 50011

²⁰Korea University, Seoul, Korea

²¹Kyungshung University, Pusan, Korea

²²Lawrence Berkeley National Laboratory and University of California, Berkeley, California 94720

²³University of Maryland, College Park, Maryland 20742

²⁴University of Michigan, Ann Arbor, Michigan 48109

²⁵Michigan State University, East Lansing, Michigan 48824

²⁶Moscow State University, Moscow, Russia

²⁷University of Nebraska, Lincoln, Nebraska 68588

²⁸New York University, New York, New York 10003

²⁹Northeastern University, Boston, Massachusetts 02115

³⁰Northern Illinois University, De Kalb, Illinois 60115

³¹Northwestern University, Evanston, Illinois 60208

³²University of Notre Dame, Notre Dame, Indiana 46556

³³University of Oklahoma, Norman, Oklahoma 73019

³⁴University of Panjab, Chandigarh 16-00-14, India

³⁵Institute for High Energy Physics, 142-284 Protvino, Russia

³⁶Purdue University, West Lafayette, Indiana 47907

³⁷Rice University, Houston, Texas 77005

³⁸Universidade Estadual do Rio de Janeiro, Brazil

³⁹University of Rochester, Rochester, New York 14627

⁴⁰CEA, DAPNIA/Service de Physique des Particules, CE-SACLAY, Gif-sur-Yvette, France

⁴¹Seoul National University, Seoul, Korea

⁴²State University of New York, Stony Brook, New York 11794

⁴³Tata Institute of Fundamental Research, Colaba, Mumbai 400005, India

⁴⁴University of Texas, Arlington, Texas 76019

⁴⁵Texas A&M University, College Station, Texas 77843

(Received 16 June 1997)

The D0 Collaboration has performed a measurement of the top quark mass m_t based on six candidate events for the process $t\bar{t} \rightarrow bW^+\bar{b}W^-$, where the W bosons decay to $e\nu$ or $\mu\nu$. This sample was collected during an exposure of the D0 detector to an integrated luminosity of 125 pb^{-1} of $\sqrt{s} = 1.8 \text{ TeV}$ $p\bar{p}$ collisions. We obtain $m_t = 168.4 \pm 12.3(\text{stat}) \pm 3.6(\text{syst}) \text{ GeV}/c^2$, consistent with the measurement obtained using single-lepton events. Combination of the single-lepton and dilepton results yields $m_t = 172.0 \pm 7.5 \text{ GeV}/c^2$. [S0031-9007(98)05457-X]

PACS numbers: 14.65.Ha, 13.85.Ni, 13.85.Qk

The pair production of top quarks has been observed in $p\bar{p}$ collisions at $\sqrt{s} = 1.8$ TeV by the CDF and D0 Collaborations [1]. Since the time of observation, the integrated luminosity has more than doubled (to 125 pb^{-1}) and the D0 experiment has substantially improved its techniques for measurement of the top quark mass m_t . We previously reported a measurement of m_t using events in which one top quark decayed semileptonically and the other decayed hadronically (the “ $\ell + \text{jets}$ ” mode, where $\ell = e$ or μ), giving $m_t = 173.3 \pm 5.6(\text{stat}) \pm 6.2(\text{syst}) \text{ GeV}/c^2$ [2]. This Letter reports a first measurement of m_t using events consistent with the $t\bar{t} \rightarrow bW^+\bar{b}W^- \rightarrow b\ell^+\nu\bar{b}\ell^-\bar{\nu}$ (“dilepton”) hypothesis. This independent measurement is important as a direct test of the hypothesis that the excess of events over background in both the $\ell + \text{jets}$ and dilepton channels is due to $t\bar{t}$ production.

The events used in this analysis were recorded by the D0 detector [3], which consists of a nonmagnetic tracking system, including a transition radiation detector (TRD), surrounded by a hermetic liquid argon/uranium calorimeter, segmented in depth into several electromagnetic (EM) and hadronic layers, and an outer toroidal muon spectrometer. Electrons are identified using a likelihood method based on the EM shower shape, track ionization, spatial match of the track with the EM shower, and TRD response. Muons are required to have reconstructed tracks in the central tracking chamber and in at least one of the spectrometer layers outside of the toroid, and to have energy deposition in the calorimeter consistent with the passage of a minimum ionizing particle. Jets are reconstructed from calorimeter energy clustered within a cone of radius $\sqrt{(\Delta\eta)^2 + (\Delta\phi)^2} = 0.5$ [4].

We select dilepton top candidate events according to criteria similar to those used in our cross section measurement [5]. This selection requires two leptons, with the transverse energy E_T of each lepton $>15(20) \text{ GeV}$ for the $e\mu$ and $\mu\mu$ (ee) channels, with $|\eta_e| < 2.5$ and $|\eta_\mu| < 1.7$, and two or more jets with $E_T > 20 \text{ GeV}$ and $|\eta| < 2.5$. For the ee and $e\mu$ channels we require significant missing transverse energy \cancel{E}_T to discriminate against background sources that have no final-state neutrinos [5], while for the $\mu\mu$ analysis we reduce the Z boson background by rejecting events for which the χ^2 probability of a fit to the $Z \rightarrow \mu\mu$ hypothesis is $>1\%$. We reject much of the remaining background using the quantities $H_T \equiv \sum_{\text{jets}} E_T$ and $H_T^e \equiv H_T + E_T(e_1)$, where all jets with $E_T > 15 \text{ GeV}$ and $|\eta| < 2.5$ enter the sum, and e_1 is the leading E_T electron. The selection requires $H_T^e(H_T) > 120(100) \text{ GeV}$ for the ee and $e\mu$ ($\mu\mu$) channels. The ee selection reported in Ref. [5] is extended to include an event that contains, in addition to an electron, one EM energy cluster without an associated reconstructed track, but with hits in the layers of the central tracking system between the interaction vertex and the cluster. This event also has a muon near

one of its jets, which is evidence of b quark decay, and further enhances the probability that the event is an example of $t\bar{t}$ production. The signal-to-background ratio for such b -tagged events in which only one of the EM clusters has an associated track is $\approx 8/1$. The final sample, therefore, consists of three $e\mu$ events, two ee events, and one $\mu\mu$ event, with expected backgrounds of 0.21 ± 0.16 , 0.51 ± 0.09 , and 0.73 ± 0.25 events, respectively (background sources are detailed in Ref. [5]). Kinematic details for the observed events can be found in Ref. [6].

We reconstruct the events according to the $t\bar{t}$ dilepton decay hypothesis. After applying the invariant mass constraints $m(\ell_1\nu_1) = m(\ell_2\nu_2) = m_W$ and $m(\ell_1\nu_1b_1) = m(\ell_2\nu_2b_2)$, the system remains underconstrained due to the two undetected neutrinos. We supply the needed additional constraints by assuming values for m_t and for two quantities associated with the neutrinos (as discussed below). We then solve for the neutrino momenta up to a fourfold ambiguity and assign a weight to each solution to characterize how likely it is to occur in $t\bar{t}$ production for the assumed m_t [7]. We compute the relative weight as a function of assumed m_t for $80 < m_t < 280 \text{ GeV}/c^2$, employing two weighting schemes with differing sensitivities to top production kinematics, decay distributions, and phase space volume consistent with the event topology.

The first weighting scheme is called matrix element weighting (\mathcal{MWT}), and is an extension of the procedure given in Ref. [8]. Here, we require the sum of the neutrino \vec{p}_T 's to equal the measured $\vec{\cancel{E}}_T$. We assign a weight

$$W_0(m_t) = A(m_t)f(x)f(\bar{x})P(E_{\ell_1}|m_t)P(E_{\ell_2}|m_t),$$

where $f(x)$ is the CTEQ3M [9] parton distribution function evaluated at the proton (antiproton) momentum fraction x (\bar{x}) required by the solution, and $P(E_\ell|m_t)$ is the probability density for the lepton energy evaluated in the top quark rest frame. The factor $A(m_t)$ normalizes the average weight of accepted events to unity, independent of the top quark mass.

The other weighting scheme, called neutrino weighting (νWT) [6], steps the assumed η for each neutrino through a range of values at each m_t . Each step spans an equal fraction of the neutrino η distribution expected in $t\bar{t}$ production. At each step a weight is assigned based on the extent to which the $\vec{\cancel{E}}_T$ measured in the event agrees with the sum of neutrino \vec{p}_T 's in the solution. The Gaussian resolution of each component of the $\vec{\cancel{E}}_T$ is 4 GeV . The weights at all η values are summed to give $W_0(m_t)$ in this method.

In calculating the consistency of the event kinematics with any given m_t , we also account for detector resolution for jets, leptons, and $\vec{\cancel{E}}_T$. This is done by fluctuating all the measured energies by their resolutions 100

(5000) times for Monte Carlo (collider data) events and summing the weights obtained for each fluctuation. The Gaussian resolutions for electrons and muons are $\sigma_E/E = 15\%/\sqrt{E}$ and $\sigma(1/p) = 0.18(p-2)/p^2 \oplus 0.003$, respectively, with E (p) in GeV (GeV/c). Jets are smeared by double Gaussians designed to model both the inherent energy resolution of the hadronic calorimeter (narrow Gaussian) and the contribution of large angle gluon radiation to the resolution (wide Gaussian). The \cancel{E}_T is then recomputed to reflect the changes in jet and lepton energies, and each component is fluctuated with a 4 GeV Gaussian.

For both the \mathcal{M} WT and ν WT methods, the up to fourfold solution ambiguity is handled by summing the weights for all solutions. Both analyses also sum over the twofold ambiguity in associating jets with leptons. Initial- and final-state gluon radiation (ISR and FSR) can create extra jets that complicate the final state. For events with extra jets, a sum is taken over all possible combinations of the three leading E_T jets, weighted by $\exp[-E_T \sin \theta_i / (25 \text{ GeV})]$ if jet i is assumed to be ISR or by $\exp[-m_{ij} / (20 \text{ GeV}/c^2)]$ if jets i and j , having invariant mass m_{ij} , are assumed to arise from the same b quark by FSR. In each case, the form of the weight is based on the characteristics of gluon radiation and the coefficient is determined empirically to maximize the sensitivity. The distributions of $W(m_t)$ [which corresponds to $W_0(m_t)$ after accounting for resolution and jet combinations] for the six candidate events, using the two weighting methods, are displayed in Fig. 1.

Because of combinatorics, and the fact that no account has been taken of background, the $W(m_t)$ distribution derived from either the \mathcal{M} WT or ν WT method cannot be considered to be a probability density. Consequently, a maximum likelihood fit is performed in which the $W(m_t)$

distributions for data are compared to the expectations from signal and background. The signal is modeled using HERWIG [10] v5.7 while the various background sources are modeled by ISAJET [11], v7.22, PYTHIA [12], and D0 data (for the instrumental backgrounds) [5].

For both analyses, the maximum likelihood fit proceeds by normalizing the $W(m_t)$ distribution for each event to unity, and integrating the fractional weights in five $40 \text{ GeV}/c^2$ bins in m_t . The first four bins form the components of a four-dimensional vector \vec{w}_i for each event i . Using the shape of the $W(m_t)$ distributions increases the statistical sensitivity of the measurement by $\approx 25\%$ over a fit to a single-valued mass estimator for each event. The likelihood $L(m_t, n_s, n_b)$ to be maximized is

$$L = g(n_b)p(n_s + n_b) \prod_i \frac{n_s f_s(\vec{w}_i | m_t) + n_b f_b(\vec{w}_i)}{n_s + n_b},$$

where n_s and n_b are the fitted signal and background levels, $g(n_b)$ is a Gaussian constraint that n_b be consistent with expectations, $p(n_s + n_b)$ is a Poisson constraint that $n_s + n_b$ be consistent with the sample size N , and f_s and f_b are the four-dimensional probability densities for signal and background. The probability densities $f(\vec{w})$ are estimated by summing four-dimensional Gaussian kernels placed at the location of \vec{w} for each event in the signal Monte Carlo (MC) or background samples [13]. Using the estimated f_s and f_b , L is maximized with respect to n_s and n_b as m_t is varied. The maximum likelihood estimate of m_t (\hat{m}_t) and its error ($\hat{\sigma}$) are determined by a quadratic fit to $-\ln L$ for the nine points about the minimum.

Applying the maximum likelihood fit to the data, we determine the top quark mass to be $m_t = 168.2 \pm 12.4 \text{ GeV}/c^2$ (\mathcal{M} WT), and $m_t = 170.0 \pm 14.8 \text{ GeV}/c^2$ (ν WT), where the uncertainties are statistical only (see Fig. 2). The results of fits to subsamples of the data are listed in Table I.

To study the properties of our mass estimator, 1000 MC “experiments” are generated by randomly selecting three $e\mu$, two ee , and one $\mu\mu$ events from simulated top (with input mass m_t^{MC}) and background samples, according to the estimated background contamination. Because of the small sample size the estimator is not normally distributed. Figure 3 shows a typical distribution for \hat{m}_t . The distribution is characterized by its median and width (half of the shortest interval that contains 68.3% of the experiments). The width of a Gaussian fit to the pull distribution $(\hat{m}_t - m_t^{\text{MC}})/\hat{\sigma}$ is consistent with unity. This verifies that $\hat{\sigma}$ is an unbiased estimate of the statistical uncertainty. The pull means can differ from zero because of the non-Gaussian tails of the \hat{m}_t distribution. Table II lists medians, widths, and means and widths of the pulls for different m_t^{MC} . The properties of \hat{m}_t are very similar for both methods.

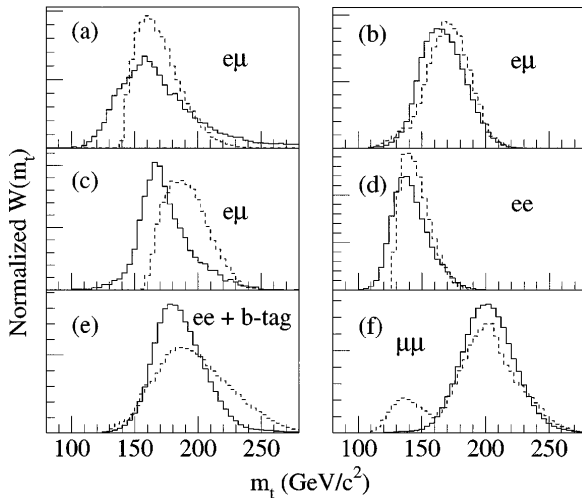


FIG. 1. $W(m_t)$ distributions for the six dilepton candidates, using the \mathcal{M} WT (dashed) and ν WT (solid) methods.

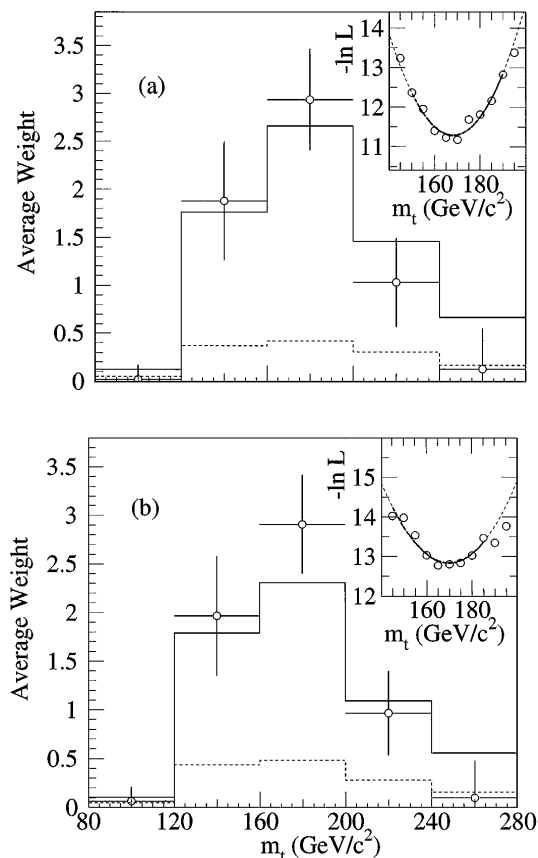


FIG. 2. Sum of the normalized candidate weights grouped into the five bins considered in the maximum likelihood fit (circles) for the (a) \mathcal{M} WT and (b) ν WT analyses. The uncertainty on these points is taken from the RMS spread of the weights in MC studies. Also shown are the average weights from the best-fit background (dashed) and signal plus background (solid). The $-\ln L$ distributions and quadratic fits are inset.

The sources of systematic uncertainty are summarized in Table III. A major uncertainty arises from the jet energy calibration, which proceeds in two steps. The first step uses γ + jets events to relate the well-calibrated electromagnetic scale to the hadronic scale. Effects considered include the overall hadronic response, energy added to jets by multiple interactions and uranium noise, and the spread of the hadronic shower outside of the jet cone [14]. The second step follows from a detailed

TABLE I. Summary of m_t measurements for full and partial data sets. Uncertainties are statistical only.

Channels fit	\mathcal{M} WT (GeV/c)	ν WT (GeV/c)
$e\mu + ee + \mu\mu$	168.2 ± 12.4	170.0 ± 14.8
$e\mu + ee$	168.0 ± 12.7	173.3 ± 14.0
$e\mu$	173.1 ± 13.3	170.1 ± 14.5

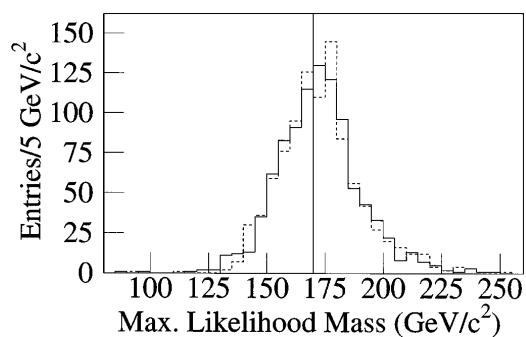


FIG. 3. Distribution of \hat{m}_t for “experiments” with $m_t^{\text{MC}} = 170 \text{ GeV}/c^2$ (marked by vertical line) using the \mathcal{M} WT (dashed) and ν WT (solid) analysis methods.

comparison of γ + jets events in MC and collider data, providing a correction that depends on jet η and ensures that the energy scale in data matches that in MC. An additional correction is applied to jets having a muon within the jet cone. Under the assumption that the muon was produced in the semileptonic decay of a heavy quark, the jet energy is increased to take into account the muon and neutrino energies. After these corrections, we find [using the γ + jets and smaller $Z(\rightarrow ee)$ + jets samples] that the data and MC scales agree, with an uncertainty of $\delta(E_T) = 0.025E_T + 0.5 \text{ GeV}$. MC tests are run on samples with the jet energies rescaled by $\pm\delta$ to yield an energy scale uncertainty of $2.4 \text{ GeV}/c^2$ in m_t .

Other sources of uncertainty arise from differences among models of $t\bar{t}$ and background production, multiple interactions, and the likelihood fit procedure. ISAJET is used as a cross-check of the HERWIG $t\bar{t}$ production model. The effect of multiple interactions is estimated using MC samples with additional random $p\bar{p}$ interactions overlaid on $t\bar{t}$ production. The contributions from all sources are summed in quadrature to give the systematic uncertainty on the measurement (see Table III).

Taking account of the 77% correlation between the \mathcal{M} WT and ν WT analyses, we measure the mass of the top quark in the dilepton channel by combining the two results:

$$m_t = 168.4 \pm 12.3(\text{stat}) \pm 3.6(\text{syst}) \text{ GeV}/c^2,$$

in good agreement with the measurement from the ℓ + jets channel [2], consistent with the $t\bar{t}$ hypothesis for both channels. We combine the results of the single- and dilepton analyses by propagating the systematic uncertainties in each channel with correlation coefficients of either zero (for MC statistics and background model) or unity (for the other systematic errors), giving

$$m_t = 172.0 \pm 5.1(\text{stat}) \pm 5.5(\text{syst}) \text{ GeV}/c^2,$$

or, combining statistical and systematic errors in quadrature, $m_t = 172.0 \pm 7.5 \text{ GeV}/c^2$.

TABLE II. Properties of the maximum likelihood estimate \hat{m}_t .

	m_t^{MC} (GeV/ c^2)	Median (GeV/ c^2)	Width (GeV/ c^2)	Pull mean	Pull width
\mathcal{M} WT	160	161.6	15.8	0.12 ± 0.03	1.03
	170	172.2	16.7	0.11 ± 0.03	0.99
	180	180.5	17.3	0.00 ± 0.03	0.98
ν WT	160	161.5	14.4	0.17 ± 0.03	0.96
	170	172.2	16.2	0.08 ± 0.03	0.98
	180	180.5	18.1	0.03 ± 0.03	1.03

TABLE III. Systematic errors in the measurement of m_t .

Source	Error (GeV/ c^2)
Jet energy scale	2.4
Signal model	1.8
Multiple interactions	1.3
Background model	1.1
Likelihood fit	1.1
Total	3.6

We thank the staffs at Fermilab and collaborating institutions for their contributions to this work, and acknowledge support from the Department of Energy and National Science Foundation (U.S.), Commissariat à l'Energie Atomique (France), State Committee for Science and Technology and Ministry for Atomic Energy (Russia), CNPq (Brazil), Departments of Atomic Energy and Science and Education (India), Colciencias (Colombia), CONACyT (Mexico), Ministry of Education and KOSEF (Korea), CONICET and UBACyT (Argentina) and the A. P. Sloan Foundation.

*Visitor from Universidad San Francisco de Quito, Ecuador.

†Visitor from IHEP, Beijing, China.

[1] CDF Collaboration, F. Abe *et al.*, Phys. Rev. Lett. **74**,

2626 (1995); D0 Collaboration, S. Abachi *et al.*, Phys. Rev. Lett. **74**, 2632 (1995).

[2] D0 Collaboration, S. Abachi *et al.*, Phys. Rev. Lett. **79**, 1197 (1997).

[3] D0 Collaboration, S. Abachi *et al.*, Nucl. Instrum. Methods Phys. Res., Sect. A **338**, 185 (1994).

[4] D0 uses a cylindrical coordinate system about the beam axis, with polar angle θ and azimuthal angle ϕ . The pseudorapidity $\eta \equiv \ln(\cot \theta/2)$ is also used.

[5] D0 Collaboration, S. Abachi *et al.*, Phys. Rev. Lett. **79**, 1203 (1997).

[6] E. W. Varnes, Ph.D. thesis, University of California, Berkeley, 1997 (unpublished) (http://www-d0.fnal.gov/publications_talks/thesis/thesis.html).

[7] K. Kondo, J. Phys. Soc. Jpn. **57**, 4126 (1988); **60**, 836 (1991).

[8] R. H. Dalitz and G. R. Goldstein, Phys. Rev. D **45**, 1531 (1992); Phys. Lett. B **287**, 225 (1992).

[9] CTEQ Collaboration, H. L. Lai *et al.*, Phys. Rev. D **51**, 4763 (1995).

[10] G. Marchesini *et al.*, Comput. Phys. Commun. **67**, 465 (1992).

[11] F. Paige and S. Protopopescu, BNL Report No. BNL38034, 1986 (unpublished).

[12] T. Sjöstrand, Comput. Phys. Commun. **82**, 74 (1994).

[13] L. Holmström, R. Sain, and H. E. Miettinen, Comput. Phys. Commun. **88**, 195 (1995).

[14] D0 Collaboration, R. Kehoe *et al.*, in *Proceedings of the 6th International Conference on Calorimetry in High Energy Physics, Frascati, 1996* (Report No. Fermilab-Conf-96/284-E).